ELSEVIER

Energy analysis of metal–metal bonding in [RM–MR]
(M = Zn, Cd, Hg; R = CH$_3$, SiH$_3$, GeH$_3$, C$_5$H$_5$, C$_5$Me$_5$)

Krishna K. Pandey *

School of Chemical Sciences, D.A. University Indore, Khandwa Road Campus, Indore 452 017, MP, India

Abstract

The metal–metal bonds of the title compounds have been investigated with the help of energy decomposition analysis at the DFT/TZ2P level. In good agreement with experiment, computations yield Hg–Hg bond distance in [H$_3$SiHg–HgSiH$_3$] of 2.706 Å and Zn–Zn bond distance in [(η^5-C$_5$Me$_5$)Zn–Zn(η^5-C$_5$Me$_5$)] of 2.281 Å. The Cd–Cd bond distances are longer than the Hg–Hg bond distances. Bond dissociation energies (-BDE) for Zn–Zn bonds in zincocene -70.6 kcal/mol in [(η^5-C$_5$H$_5$)$_2$Zn$_2$] and -70.3 kcal/mol in [(η^5-C$_5$Me$_5$)$_2$Zn$_2$] are greater amongst the compounds under study. In addition, [(η^5-C$_5$H$_5$)$_2$M$_2$] is found to have a binding energy slightly larger than those in [(η^5-C$_5$Me$_5$)$_2$M$_2$]. The trend of the M–M bond dissociation energy for the substituents R shows for metals the order GeH$_3$ < SiH$_3$ < CH$_3$ < C$_5$Me$_5$ < C$_5$H$_5$. Electrostatic forces between the metals are always attractive and they are strong (-75.8 to -110.5 kcal/mol). The results demonstrate clearly that the atomic partial charges cannot be taken as a measure of the electrostatic interactions between the atoms. The orbital interaction (covalent bonding) ΔE_{orb} is always smaller than the electrostatic attraction ΔE_{elstat}. The M–M bonding in [RM–M–R] (R = CH$_3$, SiH$_3$, GeH$_3$, C$_5$H$_5$, C$_5$Me$_5$; M = Zn, Cd, Hg) has more than half ionic character (56–64%). The values of Pauli repulsions, ΔE_{Pauli}, electrostatic interactions, ΔE_{elstat}, and orbital interactions, ΔE_{elstat} are larger for mercury compounds as compared to zinc and cadmium.
© 2006 Elsevier B.V. All rights reserved.

Keywords: Metal–metal bonding; DFT; Zinc; Cadmium; Mercury

1. Introduction

Among the Group 12 elements (Zn, Cd, Hg), compounds with metal–metal bonds are well known for mercury, reflecting the preference of mercury for a formal oxidation state of +1 [1,2]. There are more than 50 known crystal structures of dimercury compounds having a Hg–Hg bond, which are ionic and have complex oligomeric structures [3]. The two known compounds, which are considered to have a Hg(I)–Hg(I) bond, are [Hg$_2$(Me$_6$-C$_6$)$_2$][AlCl$_4$]$_2$, with Hg–Hg bond distance of 2.515 Å, [4] and the tetranuclear [(np$_3$)Co–Hg–Hg–Co(np$_3$)] complex (np$_3$ = N(CH$_2$CH$_2$PPh$_2$)$_3$) with a Hg–Hg distance of 2.651 Å [5]. Apeloig et al. reported the synthesis and the

structural characterization of [(Me$_3$SiSi–Me$_2$)$_3$Si]$_2$Hg$_2$], the first nonionic two-coordinate, dinuclear mercury(I) compound with a Hg–Hg distance of 2.6569(1) Å [6].

In sharp contrast, there are only a few compounds of the lighter metal Cd and Zn known from the literature. For cadmium, the compounds [Cd$_2$(AlCl$_4$)$_2$] [7] and [Cd$_2$(TpMe$_2$)$_2$] [8] (TpMe$_2$ = hydrotri(3,5-dimethylpyrazolyl) borate) containing Cd–Cd bonds have been synthesized and characterized. For zinc, compound HZnZnH was previously generated and characterized in matrix isolation experiments [9,10]. Until two years ago, no examples of stable, fully characterized compound with a Zn–Zn bond were known. In 2004, the group of Resa, Carmona, Gutierrraz-Puebla and Monge reported first representative example of compound containing Zn–Zn bond in decamethyldizicocene [(η^5-C$_5$Me$_5$)Zn$_2$] [11,12]. The formation of [(η^5-C$_5$Me$_5$)Zn$_2$] has been highlighted by Perkin [13] and

* Tel.: +91 7312762342; fax: +91 7312365782.
E-mail address: k_k_pandey3@rediffmail.com.

Schnepf and Himmel [14]. Robinson and coworkers have characterized the second compound with a Zn–Zn bond [R_2Zn_2] {R = [{-(2,6-Pri_2C$_6$H$_3$)N(Me)C}$_2$CH]) [15].

The quantum chemical calculations have been carried out for HZnZnH [9], X_2M_2 (X = F, Cl, Br, I; M = Zn, Cd, Hg) [16,17] 10 years earlier. All X_2M_2 are predicted to be stable against the disproportionation in the gas phase. The preparation of first stable compound containing a Zn–Zn bond, [(η^5-C$_5$Me$_5$)Zn–Zn(η^5-C$_5$Me$_5$)] has prompted theoretians and a number of excellent theoretical studies have been performed to explore the Zn–Zn bond chemistry [12,15,18–20]. Contrary to the clear information about the calculated geometries and Zn–Zn bond dissociation energies for the RZn–ZnR compounds, the discussion about the bonding situation of the Zn–Zn bond has not come to a generally accepted understanding of the nature of the chemical bond. Natural Bond Orbital (NBO) analysis of some model RZn–ZnR compounds shows charge of the zinc atoms about +0.85 e [15,20]. Often the NBO charges are not realistic, yielding too extreme values. The Hirshfeld and VDD charges, which are numerically very similar, yield chemically meaningful charges [21]. Two questions are at the center of the discussion. One question addresses the degree of covalent (orbital interactions) and ionic character (electrostatic interactions) of the Zn–Zn bonds. As Pointed out by Frenking et al., the Pauli repulsion and the electrostatic interactions must explicitly be considered in order to fully understand the bonding interactions [22]. The second question concerns whether the electrostatic interactions between Zn atoms are repulsive, because both Zn atoms carry a positive charge.

In this paper we report about an energy decomposition analysis of the nine model compounds RM–MR (R = CH$_3$, SiH$_3$, GeH$_3$) based mercury compound [(Me$_3$SiSi–Me$_2$)$_3$Si]$_2$Hg$_2$] [6] and six compounds [(η^5-C$_5$H$_5$)M–M(η^5-C$_5$H$_5$)] and [(η^5-C$_5$Me$_5$)M–M(η^5-C$_5$Me$_5$)] (M = Zn, Cd, Hg) that gives for the first time the components of bond dissociation energies that are associated with the M–M bonds. The calculations have been performed at DFT level using BP86/TZ2P.

2. Computational methods

Calculations of the model complexes have been performed at the nonlocal DFT level of theory using the exchange functional of Becke [23] and the correlation functional of Perdew [24] (BP86). Scalar relativistic effects have been considered using the ZORA formalism [25]. Uncontracted Slater-type orbitals (STOs) using triple-ζ basis sets augmented by two sets of polarization functions were employed for the SCF calculations [26]. The (1s)^2 core electrons of the carbon, (1s2s2p)^{10} core electrons of silicon and zinc, (1s2s2p3s3p)^{18} core electrons of germanium, (1s2s2p3s3p3d)^{28} core electrons of cadmium and (1s2s2p3s3p3d4s4p4d)^{46} mercury were treated by the frozen-core approximation [27]. An auxiliary set of s, p, d, f and g STOs was used to fit the molecular densities and to

present the coulomb and exchange potentials accurately in each SCF cycle [28]. The geometries of the compounds [R_2M_2] (R = CH$_3$, SiH$_3$, GeH$_3$; M = Zn, Cd, Hg) were optimized using Cs and C_{2v} symmetry and complexes [R_2M_2] (R = η^5-C$_5$H$_5$, η^5-C$_5$Me$_5$; M = Zn, Cd, Hg) were optimized using D_{5h} symmetry constraints. Geometries of the compounds were also optimized without symmetry constraints. The energy differences between the optimized structures are less than 0.10 kcal/mol, indicating a flat energy surface. The geometries of the compounds [R_2M_2] (R = CH$_3$, SiH$_3$, GeH$_3$; M = Zn, Cd, Hg) using Cs symmetry and complexes [R_2M_2] (R = η^5-C$_5$H$_5$, η^5-C$_5$Me$_5$; M = Zn, Cd, Hg) using D_{5h} symmetry constraints were found correspond to a minima on the potential energy surface. The calculations were performed utilizing the program package ADF-2005 [29].

The energy decomposition analysis for metal–metal bonds in the compounds [RM–MR] (M = Zn, Cd, Hg; R = CH$_3$, SiH$_3$, GeH$_3$, C$_5$H$_5$, C$_5$Me$_5$) between the [RM] (doublet state) radical fragments were carried out using ADF program which is based on the methods of Morokuma [30] and Ziegler and Rauk [31]. The overall bond energy ΔE between fragments is divided into two major components as:

$$\Delta E = \Delta E_{int} + \Delta E_{prep} \tag{1}$$

The preparation energy ΔE_{prep} is the amount of energy required to deform the structures of the free fragments from their equilibrium structure to geometry which they take up in the molecule:

$$\Delta E_{prep} = E_{total}(\text{distorted fragments})$$
$$- E_{total}(\text{fragments in the equilibrium structure}) \tag{2}$$

ΔE_{int} in Eq. (1) is the instantaneous interaction energy between the two fragments in the molecule. It can be decomposed into three main components:

$$\Delta E_{int} = \Delta E_{elstat} + \Delta E_{Pauli} + \Delta E_{orb} \tag{3}$$

ΔE_{elstat} describes the classical Coulomb interaction between the fragments which is attractive in most cases. The term ΔE_{Pauli}, which is called exchange repulsion or Pauli repulsion, takes into account the destabilizing two-orbital three- or four-electron interactions between occupied orbitals of both fragments. ΔE_{Pauli} is calculated by enforcing the Kohn–Sham determinant of the molecule, which results from superimposing both fragments, to obey the Pauli principle through antisymmetrization and renormalization. The last term ΔE_{orb} in Eq. (3) gives the stabilizing orbital interactions between occupied and virtual orbitals of the two fragments. ΔE_{orb} can be further partitioned into contributions by the orbitals that belong to different irreducible representations of the point group of the system.

Atomic charges were computed using the recent developed Voronoi deformation density (VDD) [32,33] and the Hirshfeld [34] scheme.

3. Results and discussion

3.1. Structures

Our computed BP86/TZ2P geometries (using a large uncontracted Slater-type orbitals (STO), no Gaussian basis functions are involved) of title compounds are presented in Fig. 1. For compounds [RM–MR] (R = CH_3, SiH_3, GeH_3; M = Zn, Cd, Hg), the trend of the M–M bond distances for the substituents R shows for metals the order $CH_3 <$ GeH_3 $< SiH_3$. The results reveal that the compounds with methyl substituent are more stable. The Hg–Hg bond distance in [$(H_3Si)_2Hg_2$] (2.706 Å) is slightly longer than the corresponding value of 2.6569(8) Å in [$(Me_3SiSi–Me_2)_3Si]_2Hg_2$]

[6]. The Hg–Si distance of 2.540 Å in [$(H_3Si)_2Hg_2$] is also slightly longer than those in [$(Me_3SiSi–Me_2)_3Si]_2Hg_2$] [6] (2.485(2) Å) and in $(Me_3Si)_2Hg$ (2.50 Å) [35]. It is important to note that the Cd–Cd bond distances are longer than the Hg–Hg bond distances, although the radii of both Cd and Hg are almost same. This can be ascribed to the fact that the quite large relativistic bond contraction is responsible for the smaller Hg–Hg bonds than the Cd–Cd bonds.

In zincocene [$(\eta^5-C_5H_5)_2Zn_2$] and [$(\eta^5-C_5Me_5)_2Zn_2$], the Zn–Zn bond lengths has been computed to be 2.291 Å and 2.281 Å, respectively. These bond lengths are slightly shorter than the experimental value 2.305(3) Å in [$(\eta^5-C_5Me_5)_2Zn_2$] and theoretically calculated in other studies [12,15,18–20]. The relativistic mass–velocity effect contracts
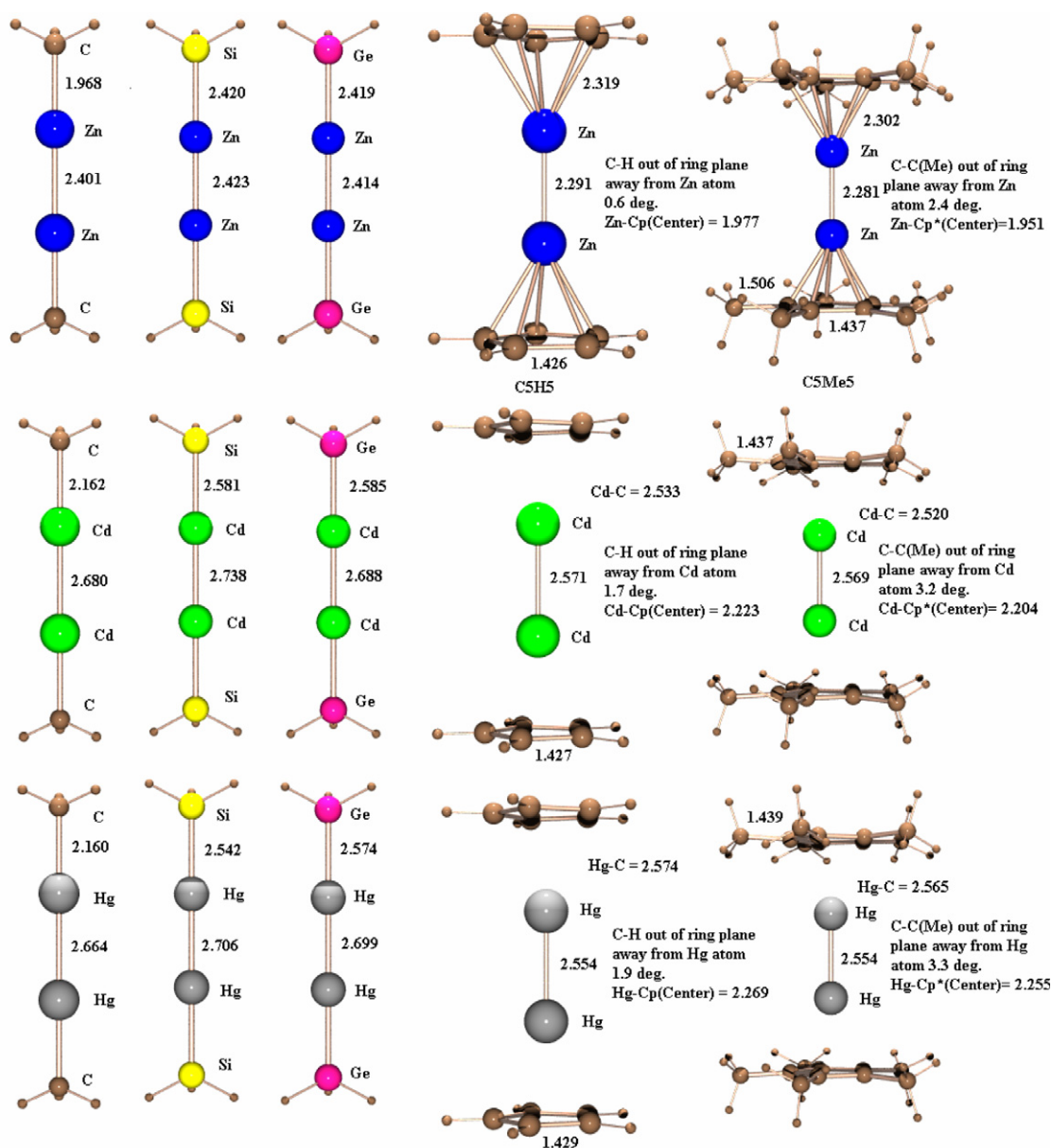

Fig. 1. Structures of [R_2M_2] (R = CH_3, SiH_3, GeH_3, C_5H_5, C_5Me_5; M = Zn, Cd, Hg). All bond distances are in Angstroms.

the M–M bonds [36] and increases slightly the bond energies (see below). As observed earlier, the Cd–Cd bond distances 2.571 Å in $[(\eta^5\text{-}C_5H_5)_2Cd_2]$ and 2.569 Å in $[(\eta^5\text{-}C_5Me_5)_2Cd_2]$ are longer than the Hg–Hg bond distances 2.554 Å in $[(\eta^5\text{-}C_5H_5)_2Hg_2]$ and 2.554 Å in $[(\eta^5\text{-}C_5Me_5)_2Hg_2]$, although the radii of both Cd and Hg are almost same.

A better explanation for the difference in M–M bond distances can be found by looking at the HOMO (singly occupied molecular orbital) of the interacting fragments [MR] (R = CH_3, SiH_3, GeH_3; M = Zn, Cd, Hg). The percentage s-character at the metal is 46.2% in $ZnCH_3$, 38.1% in $ZnSiH_3$, 38.1% in $ZnGeH_3$, 80.6% in $Zn(C_5H_5)$, 78.3% in $Zn(C_5Me_5)$; 45.4% in $CdCH_3$, 39.1% in $CdSiH_3$, 39.3% in $CdGeH_3$, 82.6% in $Cd(C_5H_5)$, 80.1% in $Cd(C_5Me_5)$ and 36.1% in $HgCH_3$, 36.2% in $HgSiH_3$, 35.1% in $HgGeH_3$, 73.4% in $Hg(C_5H_5)$, 68.9% in $Hg(C_5Me_5)$. The trends in M–M bond distances almost correspond to the percentage s-character at the metal.

3.2. Analysis of the metal–metal bonding

In the following, we try to understand the trends through detailed analyses of the electronic structure and bonding mechanism in the compounds [RM–M–R] (R = CH_3, SiH_3, GeH_3, C_5H_5, C_5Me_5; M = Zn, Cd, Hg). The results of our Kohn–Sham MO analyses are summarized in Table 1. Fig. 2 shows a diagram of the values of the repulsive term ΔE_{Pauli}, the attractive electrostatic term ΔE_{elstat}, orbital interaction term ΔE_{orb} and interaction energy ΔE_{int}. In all systems, there is a net flow of electrons from the metal to substituent R, resulting in a positive atomic charge on M according to both the VDD and the Hirshfeld method (see Table 1). The σ–electron-pair bond between the singly occupied molecular orbital of the MR fragments provides the main bonding interaction.

The calculated data shows that bond dissociation energies (-BDE) for Zn–Zn bonds in zincocene -70.6 kcal/mol in $[(\eta^5\text{-}C_5H_5)_2Zn_2]$ and -70.3 kcal/mol in $[(\eta^5\text{-}C_5Me_5)_2Zn_2]$ are greater amongst the compounds under study and also slightly greater than the reported values. In addition, $[(\eta^5\text{-}C_5H_5)_2M_2]$ is found to have a bonding energy slightly larger than those in $[(\eta^5\text{-}C_5Me_5)_2M_2]$. The trend of the M–M bond dissociation energy for the substituents R shows for metals the order $GeH_3 < SiH_3 < CH_3 < C_5Me_5 < C_5H_5$. The results reveal that the compounds with cyclopentadienyl substituent are more stable.

The results demonstrate clearly that the atomic partial charges cannot be taken as a measure of the electrostatic interactions between the atoms. Table 1 shows that the metal atoms in all compounds carry a positive charge. A naive conclusion would be that the electrostatic interactions between metal–metal are repulsive. Table 1 shows that there are strong Coulombic attractions between metals, with ΔE_{elstat} (-75.8 to -110.5 kcal/mol). The electro-

Table 1
Analysis of the Zn–Zn, Cd–Cd and Hg–Hg bonds in RM–MR (M = Zn, Cd, Hg; R = CH_3, SiH_3, GeH_3, C_5H_5, C_5Me_5) at BP86/TZ2P[a]

	RZn–ZnR					RCd–CdR					RHg–HgR				
	CH_3	SiH_3	GeH_3	C_5H_5	C_5Me_5	CH_3	SiH_3	GeH_3	C_5H_5	C_5Me_5	CH_3	SiH_3	GeH_3	C_5H_5	C_5Me_5
ΔE_σ	-55.1	-56.9	-57.7	-52.4	-51.1	-51.5	-50.6	-53.0	-49.9	-48.8	-63.3	-60.4	-60.8	-64.3	-63.3
ΔE_π	-0.8	-0.7	-0.7	-1.9	-2.4	-0.9	-1.4	-1.2	-2.6	-3.0	-0.9	-1.4	-1.5	-4.4	-4.8
ΔE_{orb}	-55.9	-57.6	-58.4	-54.3	-53.5	-52.4	-52.0	-54.2	-52.5	-51.8	-64.2	-61.8	-62.3	-68.7	-68.1
ΔE_{elstat}	-90.3	-81.2	-81.0	-87.4	-95.0	-90.4	-75.8	-81.8	-81.9	-87.6	-110.5	-93.9	-89.8	-88.4	-96.6
ΔE_{Pauli}	86.8	85.6	86.3	71.0	78.0	90.7	79.9	88.3	73.1	77.8	120.5	108.0	105.5	90.5	98.9
ΔE_{int}	-59.4	-53.2	-53.1	-70.7	-70.5	-52.1	-47.9	-47.7	-61.3	-61.6	-54.2	-47.8	-46.6	-66.6	-65.8
ΔE_{prep}	1.5	1.7	2.3	0.1	0.2	1.8	1.6	2.1	0.1	8.8	3.7	2.6	3.2	0.8	1.8
ΔE(-BDE)	-57.9	-51.5	-50.8	-70.6	-70.3	-50.3	-46.4	-45.6	-61.2	-52.8	-50.5	-45.2	-43.4	-65.8	-64.0
% I.C.[b] (%)	61.8	58.5	58.1	61.7	64.0	63.3	59.3	60.1	60.9	62.9	63.2	60.3	59.1	56.3	58.7
Metal atom charge (electron)															
VDD	0.22	0.17	0.18	0.23	0.21	0.22	0.20	0.19	0.28	0.26	0.19	0.15	0.16	0.29	0.27
Hirshfeld	0.23	0.17	0.18	0.23	0.23	0.24	0.20	0.19	0.29	0.30	0.20	0.15	0.15	0.30	0.30

[a] Energy contributions in kcal/mol.
[b] % I.C. Percentage ionic character.

static attraction ΔE_{elstat} is always greater than the orbital interaction (covalent bonding) ΔE_{orb}. The M–M bonding in [RM–M–R] (R = CH$_3$, SiH$_3$, GeH$_3$, C$_5$H$_5$, C$_5$Me$_5$; M = Zn, Cd, Hg) has more than half ionic character (56–64%). Table 1 also gives the breakdown of the ΔE_{orb} term into contributions of ΔE_σ and ΔE_π. It becomes obvious that the latter term is, in all compounds, much smaller than the σ interaction. The values of Pauli repulsions, ΔE_{Pauli}, Electrostatic interactions, ΔE_{elstat}, and orbital interactions, ΔE_{orb} are larger for mercury compounds as compared to zinc and cadmium.

Table 1 shows that the ΔE_{orb} value of the [(η^5-C$_5$Me$_5$)$_2$M$_2$] is clearly smaller than the [(η^5-C$_5$H$_5$)$_2$M$_2$]. Fig. 1 shows that M–M bond distances are shorter in [(η^5-C$_5$Me$_5$)$_2$M$_2$] than in [(η^5-C$_5$H$_5$)$_2$M$_2$] (M = Zn, Cd, Hg). We want to point out that the value of ΔE_{orb} is not simply a function of the interatomic distance. The trends observed in the bond dissociation energies are clearly reflected in the electrostatic interactions, ΔE_{elstat}, Pauli repulsions, ΔE_{Pauli}. In the compounds [(η^5-C$_5$H$_5$)$_2$M$_2$] and [(η^5-C$_5$Me$_5$)$_2$M$_2$] the Pauli repulsions are smaller and hence, the bond dissociation energy are larger.

To Visualize the Hg–Hg bonding, envelope plots of some relevant molecular orbitals of the model compound [H$_3$SiHg–HgSiH$_3$] Fig. 3. The HOMO gives a pictorial description of the Hg–Hg σ-bonding resulting from the interactions of s–p$_z$ orbital of one Hg atom and s + p$_z$ orbital of second Hg atom. The HOMO-7 is formed by the interactions of pure s orbitals of Hg atoms. HOMO-1 represents the Hg–Si bonding. LUMO and LUMO+1 are π-orbitals.
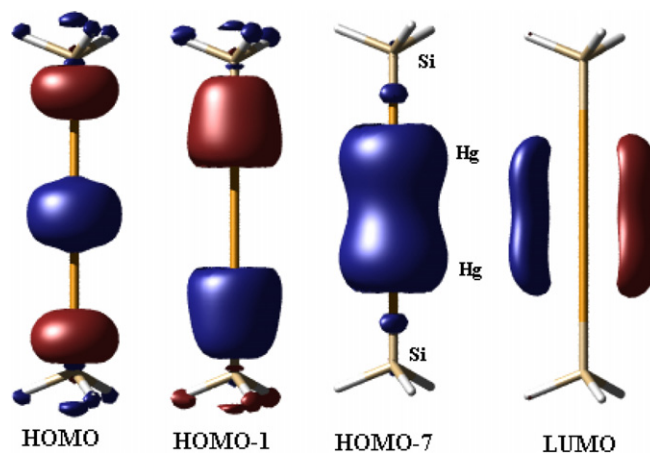

Fig. 3. Plot of some relevant orbital of [H$_3$SiHg–HgSiH$_3$].

4. Conclusion

We have presented for the first time the components of bond dissociation energies that are associated with the M–M bonds in nine model compounds RM–MR (R = CH$_3$, SiH$_3$, GeH$_3$) based mercury compound [(Me$_3$SiSi–Me$_2$)$_3$Si]$_2$Hg$_2$] and six compounds [(η^5-C$_5$H$_5$)M–M(η^5-C$_5$H$_5$)] and [(η^5-C$_5$Me$_5$)M–M(η^5-C$_5$Me$_5$)] (M = Zn, Cd, Hg). The calculated data shows that bond dissociation energies (-BDE) for Zn–Zn bonds in zincocene -70.6 kcal/mol in [(η^5-C$_5$H$_5$)$_2$Zn$_2$] and -70.3 kcal/mol in [(η^5-C$_5$Me$_5$)$_2$Zn$_2$] are greater amongst the compounds under study. The trend of the M–M bond dissociation energy for the substituents R shows for metals the order
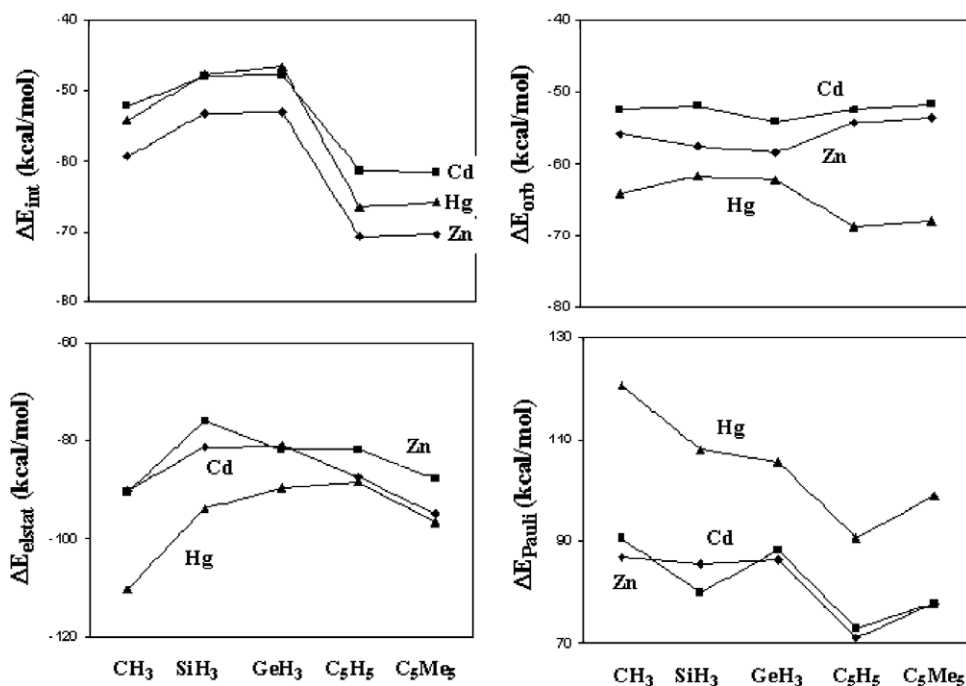

Fig. 2. Values of the interaction energy ΔE_{int}, electrostatic interactions ΔE_{elstat}, orbital interactions ΔE_{orb}, and Pauli repulsions ΔE_{Pauli} for M–M bonds in [R$_2$M$_2$].

$GeH_3 < SiH_3 < CH_3 < C_5Me_5 < C_5H_5$. The results reveal that the compounds with cyclopentadienyl substituent are more stable. The metal atoms in all compounds carry a positive charge. A naive conclusion would be that the electrostatic interactions between metal–metal are repulsive. Computed data show that there are strong Coulombic attractions between fragments, with ΔE_{elstat} (-75.8 to -110.5 kcal/mol). The results demonstrate clearly that the atomic partial charges cannot be taken as a measure of the electrostatic interactions between the atoms. The electrostatic attraction ΔE_{elstat} is always greater than the orbital interaction (covalent bonding) ΔE_{orb}. The M–M bonding in [RM–M–R] (R = CH_3, SiH_3, GeH_3, C_5H_5, C_5Me_5; M = Zn, Cd, Hg) has more than half ionic character (56–64%). M–M bond distances are shorter in [(η^5-C_5Me_5)$_2$M$_2$] than in [(η^5-C_5H_5)$_2$M$_2$], in contrast, the ΔE_{orb} values of the [(η^5-C_5Me_5)$_2$M$_2$] is clearly smaller than the [(η^5-C_5H_5)$_2$M$_2$] (M = Zn, Cd, Hg). We want to point out that the value of ΔE_{orb} is not simply a function of the interatomic distance.

Acknowledgements

References

[1] F.A. Cotton, G. Wilkinson, C.A. Murilla, M. Bochmann, Advanced Inorganic Chemistry, sixth ed., Wiley, New York, 1999.

[2] N. Wiberg (Ed.), Holleman-Wiberg Inorganic Chemistry, 101 ed., Academic Press, New York, 2001.

[3] C.E. Holloway, M. Melnic, J. Organomet. Chem. 495 (1995) 1.

[4] W. Frank, B. Dincher, Z. Naturforsch. B 42 (1987) 828.

[5] C.A. Ghilardi, S. Midollini, S.J. Moneti, Chem. Soc. Chem. Commun. (1981) 865.

[6] D. Bravo-Zhivotovskii, M. Yuzefovich, M. Bendikov, K. Klinkhammer, Y. Apeloig, Angew. Chem., Int. Ed. 38 (1999) 1100.

[7] R. Faggiani, R.J. Gillespie, J.E. Vekris, Chem. Commun. (1986) 517.

[8] D.L. Reger, S.S. Mason, A.L. Rheingold, J. Am. Chem. Soc. 115 (1993) 10406.

[9] T.M. Greene, W. Brown, L. Andrews, A.J. Downs, G.V. Chertihin, N. Runeberg, P. Pyykkö, J. Phys. Chem. 99 (1995) 7925.

[10] X. Wang, L.J. Andrews, Phys. Chem. A 108 (2004) 11006.

[11] I. Resa, E. Carmona, E. Gutierrez-Puebla, A. Monge, Science 305 (2004) 1136.

[12] D. del Río, A. Galindo, I. Resa, E. Carmona, Angew. Chem., Int. Ed. 44 (2005) 1244–1247.

[13] G. Parkin, Science 305 (2004) 1117.

[14] A. Schnepf, H.-J. Himmel, Angew. Chem., Int. Ed. 44 (2005) 3006.

[15] Y. Wang, B. Quillian, P. Wei, H. Wang, X.-J. Yang, Y. Xie, R.B. King, P.v.R. Schleyer, H.F. Schaefer III, G.H. Robinson, J. Am. Chem. Soc. 127 (2005) 11944.

[16] M. Kaupp, H.G. von Schnering, Inorg. Chem. 33 (1994) 4179.

[17] M.-S. Liao, Q.-E. Zhang, W.H.E. Schwarz, Inorg. Chem. 34 (1995) 5597.

[18] Y. Xie, H.F. Schaefer, R.B. King, J. Am. Chem. Soc. 127 (2005) 2818.

[19] Z.-Z. Xie, W.-H. Fang, Chem. Phys. Lett. 404 (2005) 212.

[20] H.S. Kang, J. Phys. Chem. A109 (2005) 4342–4351.

[21] G.C. Fonseca, J.W. Handgraaf, E.J. Baerends, F.M. Bickelhaupt, J. Comput. Chem. 25 (2004) 189.

[22] A. Diefenbach, F.M. Bickelhaupt, G. Frenking, J. Am. Chem. Soc. 122 (2000) 6449.

[23] A.D. Becke, Phys. Rev. A 38 (1988) 3098.

[24] J.P. Perdew, Phys. Rev. B 33 (1986) 8822.

[25] (a) C. Chang, M. Pelissier, Ph. Durand, Phys. Scr. 34 (1986) 394;
(b) J.-L. Heully, I. Lindgren, E. Lindroth, S. Lundquist, A.-M. Martensson-Pendrill, J. Phys. B 19 (1986) 2799;
(c) E. van Lenthe, E.J. Baerends, J.G. Snijders, J. Chem. Phys. 99 (1993) 4597;
(d) E. van Lenthe, E.J. Baerends, J.G. Snijders, J. Chem. Phys. 105 (1996) 6505;
(e) E. van Lenthe, R. van Leeuwen, E.J. Baerends, J.G. Snijders, Int. J. Quantum Chem. 57 (1996) 281;
(f) E. van Lenthe, A.E. Ehlers, E.J. Baerends, J. Chem. Phys. 110 (1999) 8943.

[26] J.G. Snijders, E.J. Baerends, P. Vernooijs, At. Data Nucl. Data Tables 26 (1982) 483.

[27] E.J. Baerends, D.E. Ellis, P. Ros, Chem. Phys. 2 (1973) 41.

[28] J. Krijn, E.J. Baerends, Fit Functions in the HFS-Method, Internal Report (in Dutch), Vrije Universiteit Amsterdam, The Netherlands, 1984.

[29] E.J. Baerends, J.A. Autschbach, A. Berces, C. Bo, P.M. Boerrigter, L. Cavallo, D.P. Chong, L. Deng, R.M. Dickson, D.E. Ellis, L. Fan, T.H. Fischer, C. Fonseca Guerra, S.J.A. van Gisbergen, J.A. Groeneveld, O.V. Gritsenko, M. Grüning, F.E. Harris, P. van den Hoek, H. Jacobsen, G. van Kessel, F. Kootstra, E. van Lenthe, V.P Osinga, S. Patchkovskii, P.H.T. Philipsen, D. Post, C.C. Pye, W. Ravenek, P. Ros, P.R.T. Schipper, G. Schreckenbach, J.G. Snijders, M. Sola, M. Swart, D. Swerhone, G. te Velde, P. Vernooijs, L. Versluis, O. Visser, E. Wezenbeek, G. Wiesenekker, S.K. Wolff, T.K. Woo, T. Ziegler, ADF, 2005, Scientific Computing and Modelling NV, The Netherlands.

[30] (a) K. Morokuma, J. Chem. Phys. 55 (1971) 1236;
(b) K. Morokuma, Acc. Chem. Res. 10 (1977) 294.

[31] (a) T. Ziegler, A. Rauk, Theor. Chim. Acta 46 (1977) 1;
(b) T. Ziegler, A. Rauk, Inorg. Chem. 18 (1979) 1558;
(c) T. Ziegler, A. Rauk, Inorg. Chem. 18 (1979) 1755.

[32] F.M. Bickelhaupt, N.J.R. van EikemaHommes, C. Fonseca Guerra, E.J. Baerends, Organometallics 15 (1996) 2923.

[33] C. Fonseca Guerra, F.M. Bickelhaupt, J.G. Snijders, E.J. Baerends, Chem. Eur. J. 5 (1999) 3581.

[34] F.L. Hirshfeld, Theor. Chem. Acta 44 (1977) 129.

[35] P. Blickmann, M. Solimann, K. Reuter, W.P. Neumann, J. Organomet. Chem. 108 (1976) C18.

[36] W.H.E. Schwarz, in: Z.B. Maksic (Ed.), The Concept of the Chemical Bond, Springer, Berlin, 1990, p. 593.